NASF SURFACE TECHNOLOGY WHITE PAPERS
88 (11), 1-6 (August 2024)

12th Quarterly Report
October-December 2023
AESF Research Project #R-122

Electrochemical Approaches to Treatment of PFAS in Plating Wastewater

by
Qingguo (Jack) Huang and Yuqing Ji*
College of Agricultural and Environmental Science
University of Georgia
Griffin, GA, USA

Editor's Note: *The NASF-AESF Foundation Research Board selected a project addressing the problem of PFAS and related chemicals in plating wastewater streams. This report covers the twelfth quarter of work (October-December 2023).*

1. Introduction

This project started in January 2021 with the goal of developing applicable electrochemical approaches to remove per- and polyfluoroalkyl substances (PFASs) present in plating wastewaters, including electrooxidation (EO) and electrocoagulation (EC). This project includes three research tasks that are designed to investigate EC, EO and EC-EO treatment train, respectively, designed to probe three hypotheses specified follows:

1) EC generates amorphous metal hydroxide flocs that can effectively adsorb PFASs in plating wastewater, which, through an appropriate treatment, can release PFASs into a concentrated solution.
2) EO enabled by a Magnéli phase Ti_4O_7 anode can be used to effectively destruct PFASs in plating wastewater.
3) The electrochemical treatment train comprised of EC and EO by Ti_4O_7 anode can remove and degrade PFASs in plating wastewater more efficiently than either process operated individually.

In our previous 11th quarterly report, we described our work on performance and effect of surface fluorinated Ti_4O_7 anodes on PFAS degradation in reactive electrochemical membrane (REM) mode. This quarter, our experiments involved utilizing porous Ti_4O_7 plates serving both as anodes and membranes. Tests compared pristine and F-18.6 Ti_4O_7 anodes at current densities of 10 mA/cm^2 and 40 mA/cm^2. The results showed immediate and sustained reduction of PFAS concentrations in the permeate. Chlorate and perchlorate generation was effectively inhibited with F-18.6 anodes. Formation of chlorate and perchlorate was minimized at lower anodic potentials (< 3.0 V_{SHE}), suggesting potential for avoiding byproduct formation in REM treatment. In this 12th quarterly report, we will discuss the mechanisms of the effects on EO performance by anode surface fluorination.

2. Experiments

Density functional theory (DFT) calculations were performed with a DMol^3 software package[1,2] in the BIOVIA Materials Studio 2020 to probe the interactions of H_2O and Cl^- with pristine and fluorinated Ti_4O_7 anodes. Double-numeric with polarization (DNP) basis sets[3] and the gradient-corrected Vosko–Wilkes–Nair–Becke–Parr (VWN-BP) functionals[4,5] were used for all calculations. For geometric optimization, the convergence tolerance for self-consistent field energy and displacement was applied at 1.0×10^{-5} Ha and 5×10^{-3} Å, respectively. Electronic convergence was set at a smearing of 0.005 Hartree (1 Hartree = 27.2114 eV) in the

* Principal Investigator (PI) Contact Information:
Qingguo Huang, Ph.D,
Professor, Department of Crop and Soil Sciences,
University of Georgia,
1109 Experiment St.,
Griffin, GA 30215, USA.
Phone: (770) 229-3302
Fax: (770) 412-4734
E-mail: qhuang@uga.edu

orbital occupation and a global orbital cutoff radius at 4.4 Å. The interactions between core and valence electrons were described using density functional semi-core pseudopotentials.[6] Implicit solvation was incorporated using COSMO polarized continuum model.[7]

A Ti_4O_7 cluster was constructed to simulate the pristine anode, which is the same model we used in our previous study.[8,9] The primary structure of a Ti_4O_7 cluster is comprised of a 2×1×1 Ti_4O_7 supercell in Magnéli phase, of which the lattice constants are a=5.638 Å, b=6.957 Å and c=7.184 Å. Terminal H atoms were used on O atoms to stabilize the clusters. The optimized supercell consists of 16 Ti ions and 28 O ions in a Ti_4O_7 cluster. The thickness of the vacuum slab was set to 30 Å.

3. Results and discussion

The study investigated the interaction between chloride ions (Cl^-) and water (H_2O) on both pristine and fluorinated Ti_4O_7 anodes through Density Functional Theory (DFT) computation. The Ti_4O_7-F, Ti_4O_7-C_7F_{15} and Ti_4O_7-$C_{13}F_{27}$ clusters were constructed (Figure 1) to explore the impact of different surface fluorination moieties. Table 1 summarizes the computed adsorption energies of Cl^- and H_2O on Ti_4O_7, Ti_4O_7-F, Ti_4O_7-C_7F_{15} and Ti_4O_7-$C_{13}F_{27}$ surfaces. The adsorption energy decreased significantly when $CF_3(-CF_2-)_n$ chain was grafted on the Ti_4O_7 surface. The adsorption of H_2O was significantly suppressed on Ti_4O_7-C_7F_{15} (-0.376 eV) and Ti_4O_7-$C_{13}F_{27}$ (-0.372 eV) surface versus Ti_4O_7 (- 1.29 eV). Therefore, surface fluorination significantly decreased the adsorption energy of Cl^- and H_2O on the anode, leading to reduced water adsorption and hydroxyl radical (OH^-) generation during electrolysis (R-1).

$$H_2O \rightarrow HO^- + H^+ + e^- \qquad \text{(R-1)}$$

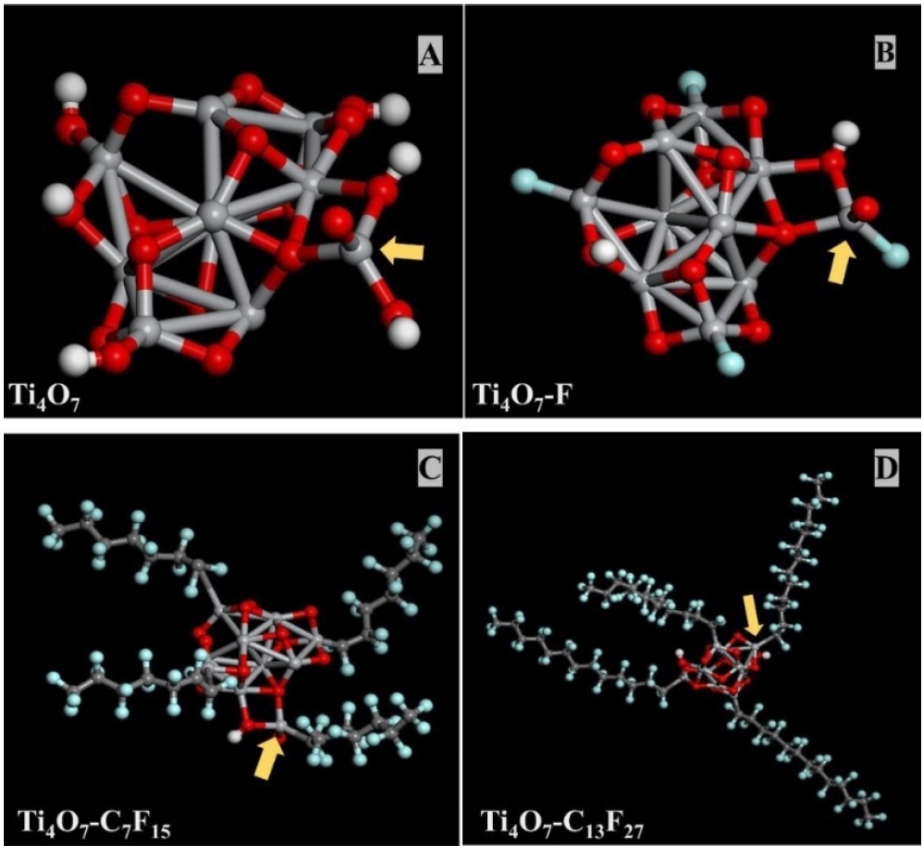

Figure 1 - Structural models of (A) a Ti_4O_7 cluster, (B) a Ti_4O_7-F cluster, (C) a Ti_4O_7-C_7H_{15} cluster and (D) a Ti_4O_7-$C_{13}H_{27}$ cluster; Color definition: Red: Oxygen; Light Gray: Titanium; White: Hydrogen; Dark grey: Carbon; Light blue: Fluorine. The yellow arrow indicates the site of adsorption for DFT computation.

Table 1 - Adsorption energies (eV) of Cl^- and H_2O on Ti_4O_7 and fluorinated-Ti_4O_7 anodes.

	Ti_4O_7	Ti_4O_7-F	Ti_4O_7-C_7F_{15}	Ti_4O_7-$C_{13}F_{27}$
Cl^-	- 4.33	- 4.02	- 3.38	- 2.42
H_2O	- 1.29	- 1.05	- 0.376	- 0.372

The reduction in OH^- concentration slowed down the degradation of PFASs like PFOS, PFOA, and 6:2 FTS, whose degradation pathways involved OH^- attack.[9,10] The proposed degradation pathways of all three PFASs are shown in Figure 2. Direct electron transfer (DET) of PFOS on the anode forms PFOS radical ($C_8F_{17}SO_3^-$) that underwent desulfurization in the presence of OH^-, and further converts to PFOA by F^- release and hydrolysis. PFOA underwent decarboxylation and CF_2-unzipping cycles to form short-chain PFAAs via DET in combination with OH^- attack, and finally decomposes to CO_2 and F^-. Unlike PFOA and PFOS, 6:2 FTS degradation was initiated by OH^- attacking nonfluorinated carbons to form PFHpA.[11] PFHpA then underwent the repeated decarboxylation and CF_2-unzipping cycles, sharing a common degradation pathway with PFOA (Figure 2).

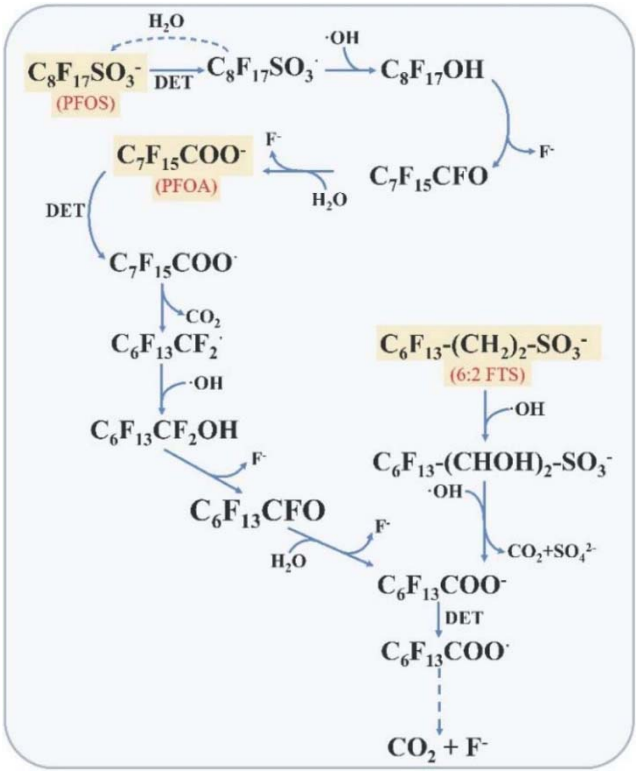

Figure 2 - Proposed degradation pathways of PFOS, PFOA and 6:2 FTS by electrooxidation.

Chlorate (ClO_3^-) and perchlorate (ClO_4^-) were formed from chloride in EO through a multistep pathway (R-2). This process was initiated by the oxidation of Cl^- to $Cl^·$, primarily via DET of Cl^- on the anode, and to less extent by OH^-oxidation.

$$Cl^- \rightarrow Cl^· \rightarrow OCL^- \rightarrow ClO_2^- \rightarrow ClO_3^- \rightarrow ClO_4^- \quad \text{(R-2)}$$

Moreover, the hypochlorite radical ($OCl^·$), the chlorite radical ($ClO_2^·$) and the chlorate radical ($ClO_3^·$) can also be generated by either DET or ·OH oxidation.[12] Therefore, indirect oxidation of Cl^- by ·OH became the primary pathway to form $Cl^·$ that initiated the process of perchlorate formation during EO. However, formation of ·OH was reduced on the fluorinated Ti_4O_7 anode because of reduced water adsorption. DFT computation also suggests that the adsorption of Cl^- on the fluorinated Ti_4O_7 anodes was also reduced. Thus, the reduced formation of ·OH on the fluorinated anodes in combination with reduced Cl^- adsorption led to effective mitigation of Cl^- oxidation to form chlorate and perchlorate in the EO systems (Figure 3).

The reduced oxidation of chloride ions (Cl^-) on fluorinated Ti_4O_7 anodes can be explained by the interfacial processes at the anode surface. Direct electron transfer (DET) of Cl^- was ineffective on both pristine and fluorinated Ti_4O_7 anodes, leading to indirect oxidation by hydroxyl radicals (·OH) as the main pathway for Cl^- oxidation, forming $Cl^·$ on the anode surface.[12] The generation of ·OH through anodic oxidation of water was significantly suppressed on fluorinated Ti_4O_7 anodes, reducing ·OH concentration near the anode surface (Figure 4). This reduction, along with the hydrophobic blocking layer created by the CF_3(-CF_2-)n chain grafted on the Ti_4O_7 surface, decreased water adsorption, ·OH generation, and restricted their diffusion. Consequently, both reduced ·OH generation and lower Cl^- concentration near the anode surface led to mitigated formation of chlorate and perchlorate.

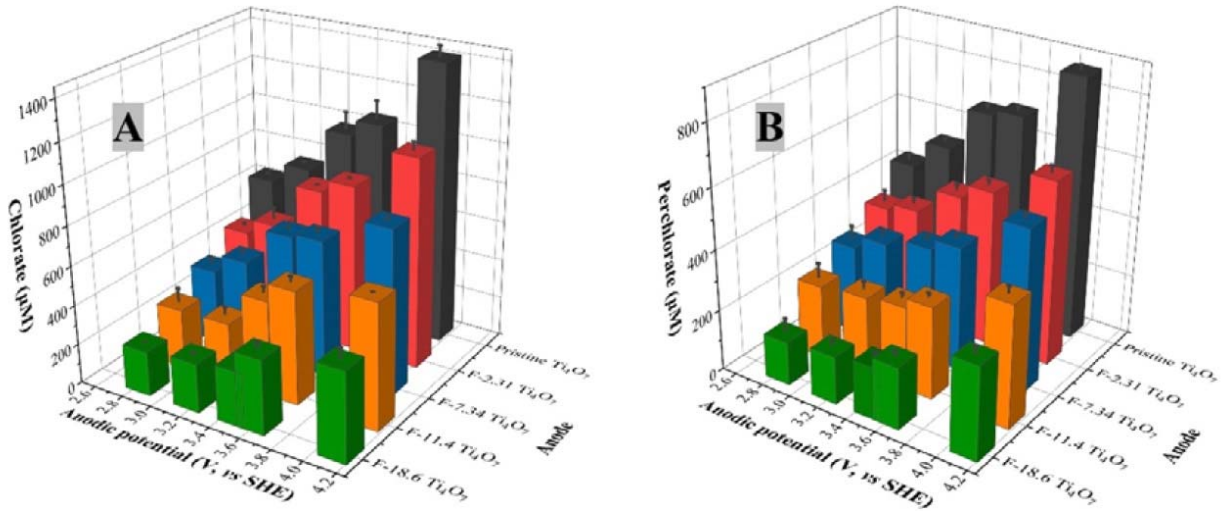

Figure 3 - The concentration of chlorate (A) and perchlorate (B) at different anodic potentials on pristine and fluorinated Ti_4O_7 anode at 8-hour electrooxidation. Initial PFAS concentration: 2 μM, supporting electrolyte: 100-mM Na_2SO_4 + 10-mM NaCl. Error bar represents standard deviations of replicates.

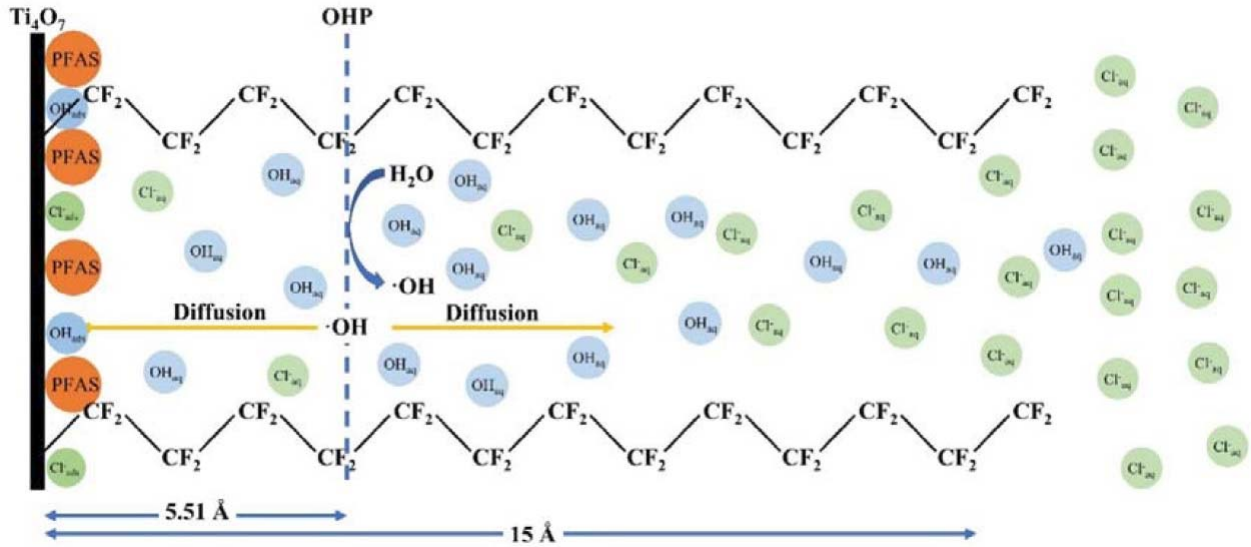

Figure 4 - Schematic of proposed mechanism of Cl^- oxidation of ~~and~~ fluorinated Ti_4O_7 anode.

4. References

1. B. Delley, "An all-electron numerical method for solving the local density functional for polyatomic molecules," *Journal of Chemical Physics,* 92, 508-517 (1990); https://doi.org/10.1063/1.458452
2. B. Delley, "From molecules to solids with the DMol^3 approach," *Journal of Chemical Physics*, 113, 7756-7764 (2000); https://doi.org/10.1063/1.1316015
3. B. Delley, "Fast Calculation of Electrostatics in Crystals and Large Molecules," *Journal of Physical Chemistry*, 100 (15), 6107-6110 (1996); https://doi.org/10.1021/jp952713n
4. S.H. Vosko, L. Wilk, and M. Nusair, "Accurate spin-dependent electron liquid correlation energies for local spin density calculations: a critical analysis," *Canadian Journal of Physics*, 58 (8), 1200-1211 (1980); https://doi.org/10.1139/p80-159
5. A.D. Becke, "A multicenter numerical integration scheme for polyatomic molecules," *Journal of Chemical Physics*, 88 (4), 2547-2553 (1988); https://doi.org/10.1063/1.454033

6. B. Delley, "Hardness conserving semilocal pseudopotentials," *Physical Review B*, 66 (15), 155125 (2002); https://doi.org/10.1103/PhysRevB.66.155125
7. A.S. Dukhin, and P.J. Goetz, "Chapter 2 - Fundamentals of Interface and Colloid Science," in: A.S. Dukhin, and P.J. Goetz (Eds.), *Characterization of Liquids, Dispersions, Emulsions, and Porous Materials Using Ultrasound* (Third Edition), Elsevier, (2017); pp. 19-83.
8. A. Klamt, and G. Schüürmann, "COSMO: a new approach to dielectric screening in solvents with explicit expressions for the screening energy and its gradient," *Journal of the Chemical Society: Perkin Transactions*, 2, 799-805 (1993); https://doi.org/10.1039/P29930000799
9. H. Shi, Y. Wang, C. Li, R. Pierce, S. Gao, and Q. Huang, "Degradation of Perfluorooctanesulfonate by Reactive Electrochemical Membrane Composed of Magnéli Phase Titanium Suboxide," *Environmental Science & Technology*, 53 (24), 14528-14537 (2019); https://doi.org/10.1021/acs.est.9b04148
10. J. Radjenovic, N. Duinslaeger, S.S. Avval, and B.P. Chaplin, "Facing the Challenge of Poly- and Perfluoroalkyl Substances in Water: Is Electrochemical Oxidation the Answer?" *Environmental Science & Technology* 54 (23), 14815-14829 (2020); https://doi.org/10.1021/acs.est.0c06212
11. Q. Zhuo, X. Li, F. Yan, B. Yang, S. Deng, J. Huang, and G. Yu, "Electrochemical oxidation of 1H,1H,2H,2H-perfluorooctane sulfonic acid (6:2 FTS) on DSA electrode: Operating parameters and mechanism," *Journal of Environmental Sciences*, 26 (8), 1733-1739 (2014); https://doi.org/10.1016/j.jes.2014.06.014
12. L. Wang, J. Lu, L. Li, Y. Wang, and Q. Huang, "Effects of chloride on electrochemical degradation of perfluorooctanesulfonate by Magnéli phase Ti_4O_7 and boron doped diamond anodes," *Water Research*, 170, 115254 (2020a); https://doi.org/10.1016/j.watres.2019.115254

5. Past project reports

1. Introduction to Project R-122: Summary: *NASF Report* in *Products Finishing*; *NASF Surface Technology White Papers*, 85 (6), 13 (March 2021); Full paper: http://short.pfonline.com/NASF21Mar1.
2. Quarter 1 (January-March 2021): Summary: *NASF Report* in *Products Finishing*; *NASF Surface Technology White Papers*, 85 (12), 13 (September 2021); Full paper: http://short.pfonline.com/NASF21Sep1.
3. Quarter 2 (April-June 2021): Summary: *NASF Report* in *Products Finishing*; *NASF Surface Technology White Papers*, 86 (3), 18 (December 2021); Full paper: http://short.pfonline.com/NASF21Dec2.
4. Quarter 3 (July-September 2021): Summary: *NASF Report* in *Products Finishing*; *NASF Surface Technology White Papers*, 86 (6), 16 (March 2022); Full paper: http://short.pfonline.com/NASF22Mar2.
5. Quarter 4 (October-December 2021): Summary: *NASF Report* in *Products Finishing*; *NASF Surface Technology White Papers*, 86 (9), 21 (June 2022); Full paper: http://short.pfonline.com/NASF22Jun2.
6. Quarter 5 (January-March 2022): Summary: *NASF Report* in *Products Finishing*; *NASF Surface Technology White Papers*, 86 (12), 22 (September 2022); Full paper: http://short.pfonline.com/NASF22Sep2.
7. Quarter 6 (April-June 2022): Summary: *NASF Report* in *Products Finishing*; *NASF Surface Technology White Papers*, 87 (3), 17 (December 2022); Full paper: http://short.pfonline.com/NASF22Dec1.
8. Quarter 7 (July-September 2022): Summary: *NASF Report* in *Products Finishing*; *NASF Surface Technology White Papers*, 87 (6), 19 (March 2023); Full paper: http://short.pfonline.com/NASF23Mar2.
9. Quarter 8 (October-December 2022): Summary: *NASF Report* in *Products Finishing*; *NASF Surface Technology White Papers*, 87 (9), 19 (June 2023); Full paper: http://short.pfonline.com/NASF23Jun1.
10. Quarter 9 (January-March 2023): Summary: *NASF Report* in *Products Finishing*; *NASF Surface Technology White Papers*, 87 (12), 17 (September 2023); Full paper: http://short.pfonline.com/NASF23Sep2
11. Quarter 10 (April-June 2023): Summary: *NASF Report* in *Products Finishing*; *NASF Surface Technology White Papers*, 88 (5), 19 (February 2024); Full paper: http://short.pfonline.com/NASF24Feb2
12. Quarter 11 (July-September 2023): Summary: *NASF Report* in *Products Finishing*; *NASF Surface Technology White Papers*, 88 (8), 15 (May 2024); Full paper: http://short.pfonline.com/NASF24May2

6. About the principal investigator

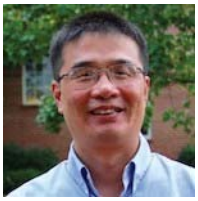

Qingguo (Jack) Huang is Professor in the Department of Crop and Soil Sciences, University of Georgia, Griffin Campus. He holds a B.S. in Environmental Science (1990) and a Ph.D. in Chemistry (1995) from Nanjing University, China as well as a Ph.D. in Environmenal Engineering from the University of Michigan, Ann Arbor, Michigan. Dr. Huang's research interest focuses on catalysis involved in the environmental transformation of organic pollutants, and development of catalysis-based technology for pollution control and environmental remediation and management. His laboratory has been actively involved in several cutting-edge research topics:

- Enzyme-based technology for water/wastewater treatment and soil remediation
- Electrochemical and reactive electrochemical membrane processes in wastewater treatment
- Catalysis in biofuel production and agro-ecosystem management
- Environmental fate and destructive treatment methods of PFASs
- Environmental application and implication of nanomaterials

He has published over 170 peer-reviewed journal articles, five book chapters and had six patents awarded. He has taught three courses at the University Georgia: *Introduction to Water Quality*, *Environmental Measurement* and *Advanced Instrumental Analysis in Environmental Studies*.